A Study on Planning for Interconnected Renewable Energy Facilities in Hokkaido, Japan

Shin'ya Obara, Power Engineering Laboratory, Department of Electrical and Electronic Engineering, Kitami Institute of Technology, Koen-cho 165, Kitami, Hokkaido 090-8507, Japan
Phone/FAX: +81-157-26-9262, e-mail: obara@mail.kitami-it.ac.jp

Yuta Utsugi, Power Engineering Laboratory, Department of Electrical and Electronic Engineering, Kitami Institute of Technology

Yuzi Ito, Power Engineering Laboratory, Department of Electrical and Electronic Engineering, Kitami Institute of Technology

Jorge Morel, Power Engineering Laboratory, Department of Electrical and Electronic Engineering, Kitami Institute of Technology

Masaki Okada, Department of Mechanical Systems Engineering, National Institute of Technology, Asahikawa College, Shyunkodai 2-2-1-6, Asahikaw, Hokkaido 071-8142, Japan

Abstract

In this paper, to optimize the kind and capacity of renewable energy installed in each area, an optimization program was developed using a simple genetic algorithm (GA). In the proposed algorithm, the kind and capacity of renewable energy was expressed using a chromosome model. The most efficient and economical system could be identified by applying the model in a random computer search. A case study was developed to test the proposed algorithm. In the case study, a solar power station was installed near 14 cities in Hokkaido, Japan, and a wind power station was installed seven areas. Using the algorithm, the system planning requirements for the

interconnection of these renewable energy facilities over a large area were optimized. On the basis of these results, the kind and capacity of renewable energy considered to be the most economically advantageous to the region were identified and evaluated. Using the proposed optimization algorithm for planning and design, an efficient, economical, and interconnected system of electrical power could be realized from renewable energy over a large area.

Key Words: renewable energy, power grid, interconnection, arrangement optimization, power stabilization

1. Introduction

To expand controls on the discharge of greenhouse gases and the use of safe power sources, it is necessary to encourage the interconnection of a large quantity of renewable energy in commercial electric power networks. However, the cost of equipment for backup power supply and energy storage for stabilizing fluctuations in power output is a vital concern in the renewable energy industry. Many studies have reported on techniques for controlling and stabilizing power fluctuations in renewable energy [1-9] along with methods for backup power supply [10-15]. Furthermore, new technologies for optimizing energy management and operational planning [16-19], and microgrid based on extensive introduction of renewable energy [20-22] have also been investigated. In general, a change in the power output of several minutes or less is defined as a cyclic fluctuation, e.g., a change in weather. A change in power output from several minutes to about 20 minutes is defined as a fringe fluctuation, e.g., a change in the relative position of the sun. Finally, a change in power output exceeding 20 minutes is

defined as a sustained fluctuation, e.g., seasonal changes in weather patterns that affect the output of solar or wind energy facilities. In the case of wind power, a cyclic fluctuation may be a change in wind speed, a fringe fluctuation may include changes in wind direction from morning to evening, and a sustained fluctuation may include seasonal changes in the direction and speed of prevailing winds [23-28].

When solar and wind power generation facilities are interconnected over a large area, fluctuations in the power output of one facility may be offset by the sustained output of another [29, 30]. For example, when two or more solar power stations that are located several kilometers apart are interconnected, the cyclic fluctuation of each power station can be smoothed [29]. Moreover, when wind power stations located in areas with different wind speed characteristics are interconnected, fringe and cyclic fluctuations can be smoothed [30]. Therefore, when solar and wind power stations are installed in a large area and interconnected at a suitable rate, a wide range of potential power fluctuations (cyclic to sustained) can be smoothed. Moreover, when power output is smoothed by interconnecting renewable energy facilities over a large area, the cost to stabilize the supply of electricity can decrease significantly. However, to achieve this goal, it is necessary to clarify the type and rated capacity of the renewable energy facilities. Therefore, the objective of this study was to develop a computer algorithm that identifies the most economically advantageous power source when solar and wind power stations are interconnected over a large area. In the proposed genetic algorithm (GA), many power sources with nonlinear characteristics and variables can be managed [31-34]. The GA offers a method of conducting random computerized searches with high efficiency. It can identify solutions for optimizing power output in which industrial applications are possible. When the algorithm

optimizes the configuration of renewable energy facilities based on economical efficiency, it reflects the characteristics of climatic conditions and demand for electricity in each area. As a result, the findings of this study can contribute toward the planning and designing of renewable energy power generating systems that are interconnected over large areas.

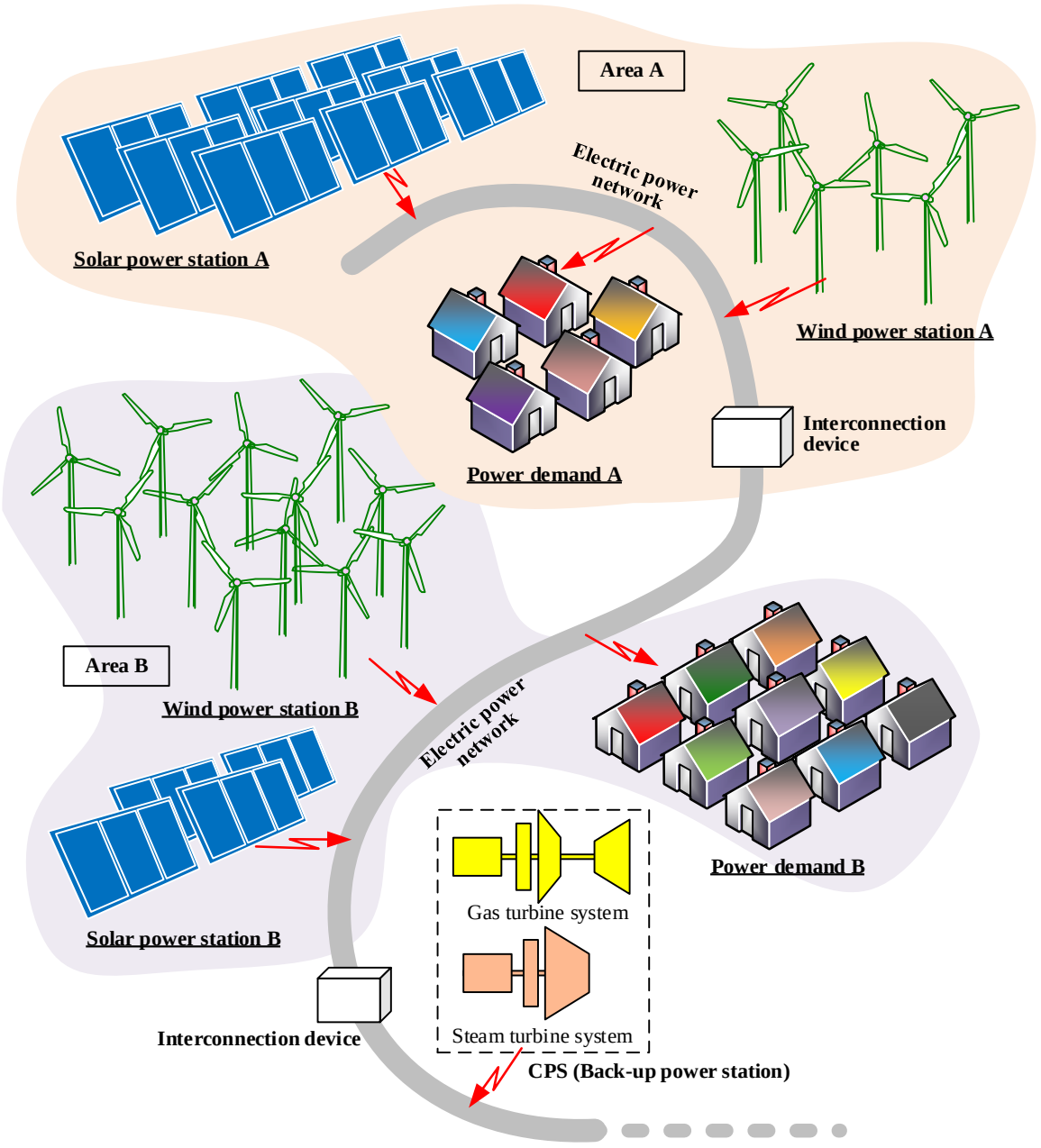

Fig. 1 The proposed power supply network for the interconnection of renewable energy facilities over a large geographical area

2. System Scheme

2.1 Distributed power supply network

Figure 1 shows an example of the proposed power supply network for the interconnection of renewable energy facilities over a large geographical area. In the example, solar and wind power stations are installed in Areas A and B, respectively. In addition, a Controllable Power Source of Output Power (CPS) backup power station is installed. Power consumption in Area A (Power demand A) is supplied by solar power station A and wind power station A, while power consumption in Area B (Power demand B) is supplied by solar power station B and wind power station B. The electrical power grids in Areas A and B are connected through an interconnection device, and have the potential to reach areas located farther away. Electrical power from the proposed system can be supplied to other areas through the electrical power grids. Furthermore, the CPS provides a reliable supply of backup power to offset periodic fluctuations in renewable energy power output.

2.2 Electrical supply and demand of the proposed system

2.2.1 Supply and demand characteristics of each area

A solar power station and wind power station are installed for supplying electricity to one area. When power output exceeds demand, electricity remains in the area; surplus electricity can be supplied to other areas or the interconnection of some power sources is removed. On the other hand, when demand for electricity exceeds power output, surplus power can be transferred from other areas or from the CPS. Although thermal power or hydroelectric power are assumed to be the sources of energy for the CPS, cost corresponds to the production of electricity. In this

study, the pattern of supply and demand for electrical power is applied to all the areas in the electrical power system. The capacity of solar power stations, wind power stations, and the CPS is optimized. This, in turn, minimizes the cost of delivery through power interchanges between areas and results in an economical and efficient power distribution system.

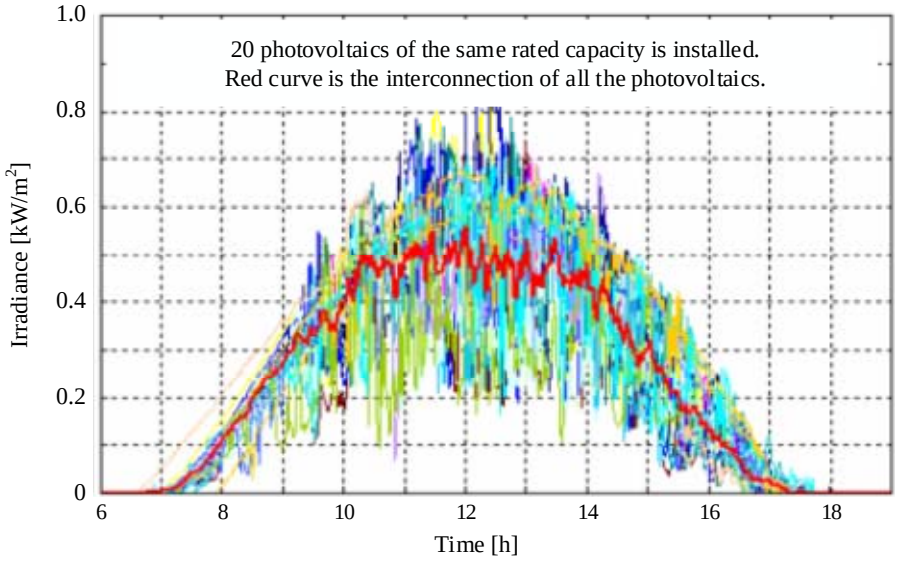

Fig. 2 The amount of global solar radiation received by 20 global solar radiation meters [29]

2.2.2 Control of power fluctuations by interconnection of renewable energy facilities

Figure 2 shows the amount of global solar radiation received by 20 global solar radiation meters [29]. Each colored curve represents the test results from one of the 20 meters. The red curve represents the total power output of all the 20 meters at any given time during the test. The maximum power fluctuation at any one of the meters was approximately 70% of the rated power in 10 seconds. However, when all the 20 meters were interconnected, power fluctuations were reduced to 20% or less of rated power. The effect was to smooth the cyclic fluctuations in power output to less than 10 seconds.

The rate of output fluctuation of wind power generation was defined by the ratio of output fluctuations to installed capacity, as shown in Eq. (1). When the amount of interconnection of wind power generation was increased, the rate of fluctuation decreased because of leveling; however, the amount of fluctuation increased. The reason for this increase was the similarity in climatic conditions at various facility sites, even when they were located hundreds of km apart. As the correlation between site climatic conditions increased, fluctuations increased proportionally. The fringe fluctuation resulting from the interconnection of wind power generation facilities was 23% of the rated power [30].

$$r_{pf,wp} = \frac{p_{pf,wp}}{V_{wp}} \times 100 \quad (1)$$

3. Analysis Method

3.1 Electrical power balance

Equation (2) shows the power balance equation for the proposed system. The left side of the equation contains each term of power supply, and the right hand side contains each term of power consumption. Power supplies include solar power stations, wind power stations, supplemental power from other areas, and a CPS. Power consumption includes electrical demand of the area, transmission of power to other areas, and power loss. In Eq. (2), the power transmitted to Area m from Area i is expressed by $\Delta p_{tp,i\to m}$, and $\Delta p_{loss,i\to m}$ shows transmission loss. Because all power generation facilities in the area are interconnected through the power grid, it is necessary to satisfy the power balance for the entire proposed system.

$$\sum_{i=1}^{N_{area}} \left(\sum_{j=1}^{N_{pv}} p_{pv,i,j} + \sum_{k=1}^{N_{wp}} p_{wp,i,k} + \sum_{l=1}^{N_{tp}} p_{tp,i,l} \right) + p_{cps} = \sum_{i=1}^{N_{area}} \left\{ \Delta p_{need,i} + \sum_{m=1}^{N_{area}} \left(\Delta p_{tp,i \to m} + \Delta p_{loss,i \to m} \right) \right\} \quad (2)$$

3.2 Cost analysis

Equations (3) and (4) represent the equipment and fuel costs of the proposed system, respectively. The cost C_{pv} , C_{wp} , C_{cps} of each type of equipment is obtained by multiplying the rated capacity V by the equipment unit price u . Moreover, the fuel cost is obtained by multiplying fuel consumption v_{cps} of the CPS by the unit fuel price u_{fuel} and the operating period N_{period}. Because the power generation efficiency of a power source changes with load factor, the fuel consumption v_{cps} is calculated using the rated power V_{cps} and the mean power generation efficiency $\overline{\eta}_{cps}$ during the operating period. In the equation, t and Δt represent sampling time and sampling time intervals, respectively.

$$C_{equipment} = \sum_{i=1}^{N_{area}} \left(\sum_{j=1}^{N_{pv}} C_{pv,i,j} + \sum_{k=1}^{N_{wp}} C_{wp,i,k} \right) + C_{cps} = \sum_{i=1}^{N_{area}} \left(\sum_{j=1}^{N_{pv}} u_{pv} \cdot V_{pv,i,j} + \sum_{k=1}^{N_{wp}} u_{wp} \cdot V_{wp,i,k} \right) + u_{cps} \cdot V_{cps} \quad (3)$$

$$C_{fuel,period} = \sum_{t=0}^{N_{period}} \left(u_{fuel} \cdot v_{cps,i} \cdot \Delta t \right) = \sum_{t=0}^{N_{period}} \left(u_{fuel} \cdot \frac{V_{cps}}{\overline{\eta}_{cps}} \cdot \Delta t \right) \quad (4)$$

3.3 Transmission loss

The loss of power during transmission between areas is the product of the amount of power transmitted $\Delta p_{tp,i \to m}$, the transmission distance $l_{i \to m}$, and the loss factor λ_{loss} , as shown in Eq. (5).

$$\sum_{t=0}^{N_{period}} \sum_{i=1}^{N_{area}} \sum_{m=1}^{N_{area}} \left(\Delta p_{loss,t,i\to m}\right) = \sum_{t=0}^{N_{period}} \sum_{i=1}^{N_{area}} \sum_{m=1}^{N_{area}} \left(\Delta p_{tp,t,i\to m} \cdot l_{i\to m} \cdot \lambda_{loss}\right) \quad (5)$$

When delivering electrical power $\Delta p_{tp,t,i}$ from Area i to another area, the cost of delivery using the delivery unit price u_{dv} is calculated by Eq. (6)

$$C_{tp,\,period} = \sum_{i=1}^{N_{area}} \sum_{t=0}^{N_{period}} \left(\Delta p_{tp,t,i} \cdot u_{dv} \cdot \Delta t\right) \quad (6)$$

3.4 Analysis procedure

3.4.1 Objective function

Equation (7) is the objective function of the proposed system, which is expressed as the sum of the equipment cost $C_{equipment}$, fuel cost $C_{fuel,\,period}$, and the cost of delivery $C_{tp,\,period}$ to other areas. In the equation, the system configuration represents the minimum optimal solution for the proposed system.

$$F_{system} = C_{equipment} + C_{fuel,\,period} + C_{tp,\,period} \quad (7)$$

3.5 Analysis flow

3.5.1 Planning of the distributed power supply network

Because weather conditions are different in every area, the type and rated capacity of the power distribution system to be installed in each area are planned. When the size of the system increases, analysis requires a method in which two or more power sources with nonlinear

characteristics can be simultaneously optimized. Therefore, the analysis will depend on the GA, which can simultaneously analyze many nonlinear variables.

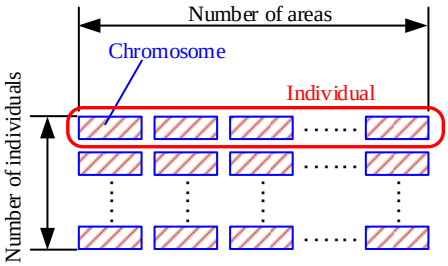

(a) Composition of a chromosome model

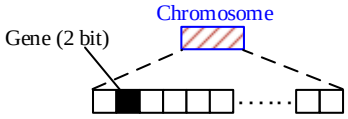

(b) Composition of a gene model

Fig. 3 Chromosome model

3.5.2 Optimizing analysis using the genetic algorithm

(1) Chromosome model

Figure 3 shows the chromosome model introduced into the GA. An individual, as shown in Fig. 3(a), consists of groups of chromosomes representing the power output of all the renewable energy facilities in an entire area. A chromosome consists of two-bit gene clusters of 0 and 1, as shown in Fig. 3(b). Several individuals are randomly generated by a computer, and the adaptive value of each individual is calculated. The individual that satisfies the value of the objective function, Eq. (7), is identified as a solution with high adaptive value. The individual with high adaptive value is proliferated and the individual with low individual is selected (selection operation). Genetic manipulation of individuals is repeated and an individual with the highest adaptive value is identified as the optimal solution by the final generation. The rated power of

solar or wind power stations to serve the area is determined by decoding chromosomes for the optimal solution. Details of the analysis flow are provided below.

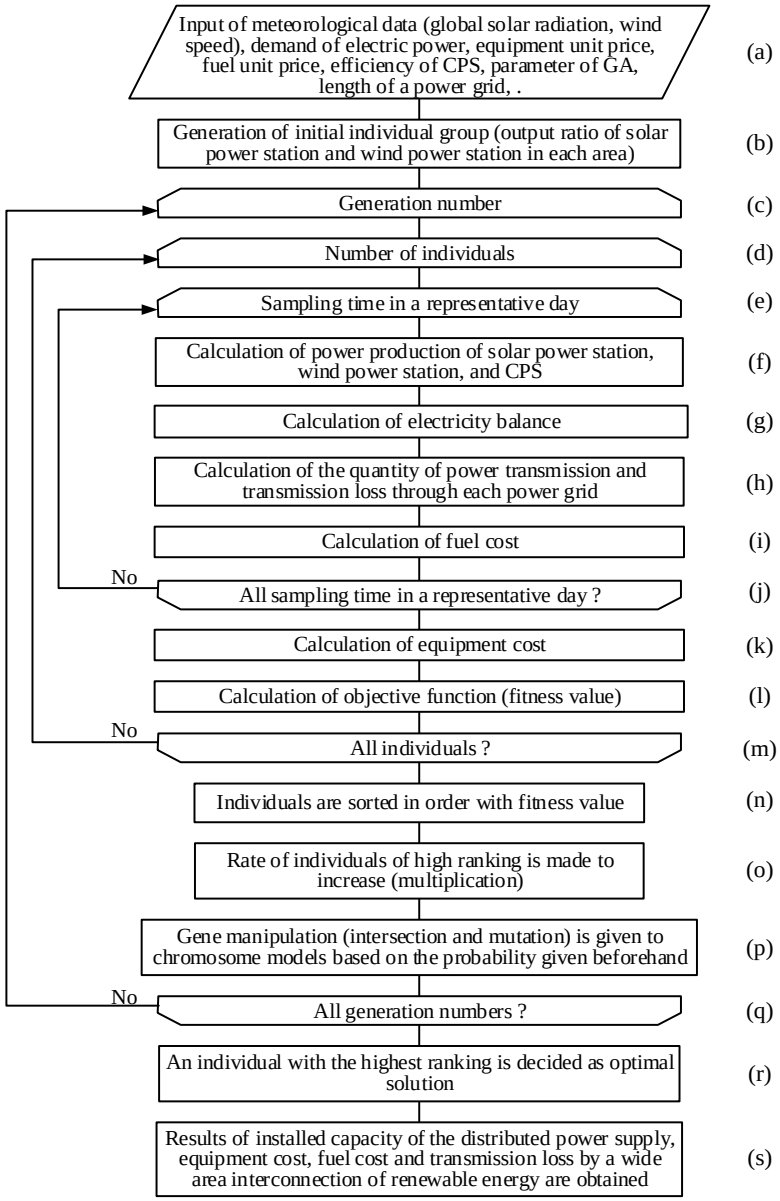

Fig. 4 The analysis flow of the proposed algorithm

(2) Flow of the analytic algorithm

Figure 4 shows the analysis flow of the proposed algorithm. Initial data, assumptions, etc. are identified in step (a), and several initial chromosome models (individuals) are randomly

prepared in step (b). By repeating the calculations in steps (e) through (j), the power output of the solar or wind power stations derived with the chromosome model is inserted into the power balance Eq. (2). For every sampling time, the power generated by the CPS, power transmitted over interchanges, and transmission loss ((Eq. (5)) are calculated in steps (f) through (h). For every sampling time, fuel consumption of CPS is calculated in step (i) using Eq. (4). The calculations in steps (e) through (j) are conducted for all the individuals ((d) through (m)), and the cost of equipment for each individual is calculated in step (k) using Eq. (3). The high adaptive individuals are then sequentially arranged by value in step (n). Next, in step (l), the objective function is calculated using Eq. (7) and the adaptive value of all the individuals is determined. In step (n), individuals are again sequentially arranged by adaptive value.

Step (o) is a selection operation in which an individual group with high adaptive value is increased, and the group of low individuals is selected. In step (p), the crossover and mutation operations are added to some chromosome groups, and the diversity of the chromosome model group is maintained as much as possible. In the crossover operation, two parent chromosomes are extracted, each containing a solar and wind power station in an individual according to the probability given previously. The gene cluster in front and behind the random gene in the parent is replaced. Mutation is initiated by reversing the random gene in a chromosome according to the probability given previously.

Calculations in steps (d) through (p) are repeated according to the generation number given previously ((c) to (q)). As an optimal solution in a final generation's chromosome group, an individual with the highest adaptive value is extracted. By decoding the gene in the chromosome of the optimal solution, the following are obtained: power output capacity of the solar and wind

power stations for the entire area, power output capacity of the CPS, amount of fuel consumption, amount of power transmitted through interchanges, and transmission loss.

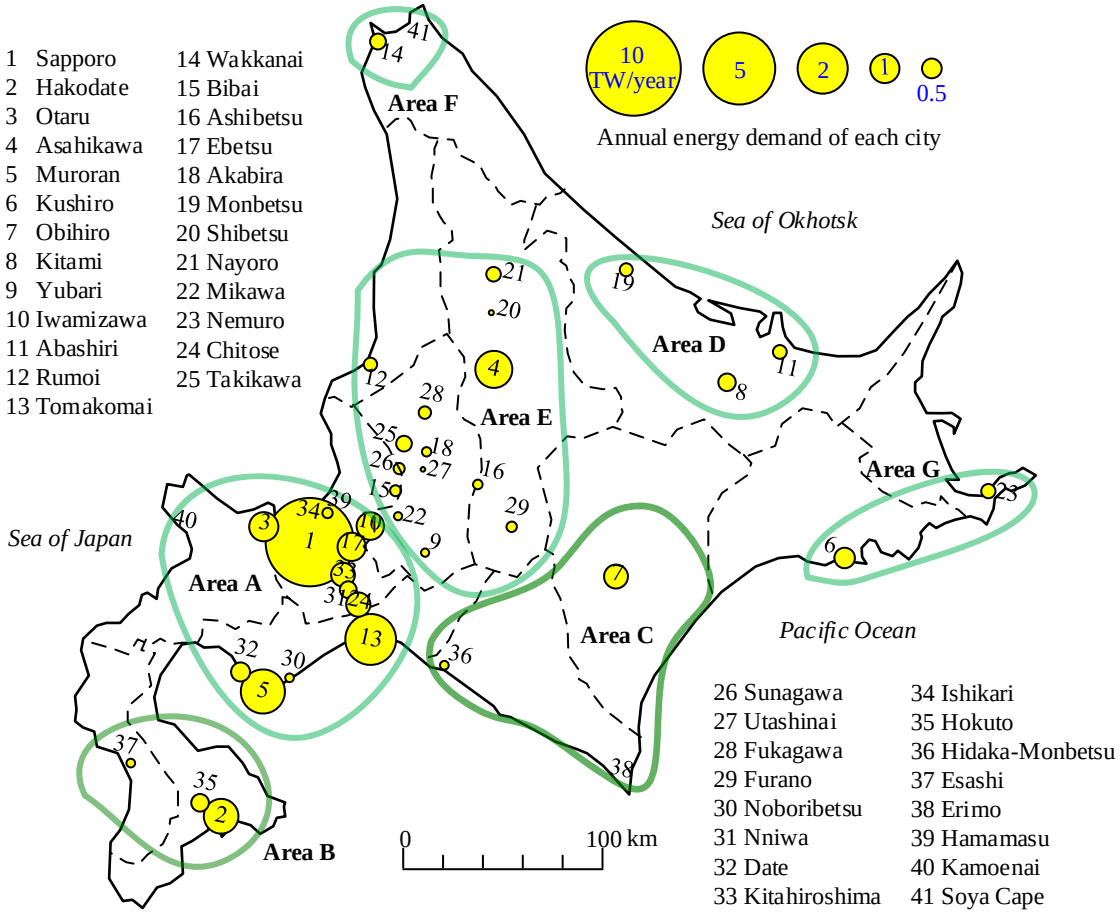

Fig. 5 The principal cities in Hokkaido, Japan and their annual energy demand. Hokkaido

4. Example for Analysis

4.1 Electrical power system

4.1.1 The Hokkaido electrical power system

Figure 5 shows the principal cities in Hokkaido, Japan and their annual energy demand. Hokkaido is spread over an area of 83,450 km² with a population of 5,460,000 and 2,720,000 households. The climate of Hokkaido is generally cold. The difference between summer and

winter temperatures is large, and the region experiences heavy snowfall. Approximately 81% Hokkaido's population resides in the city numbered 1 to 35 shown in Fig. 5. Considering the weather characteristics and population distribution of Hokkaido, each city can be assigned to one of the seven areas, indicated within the green lines as areas A to G.

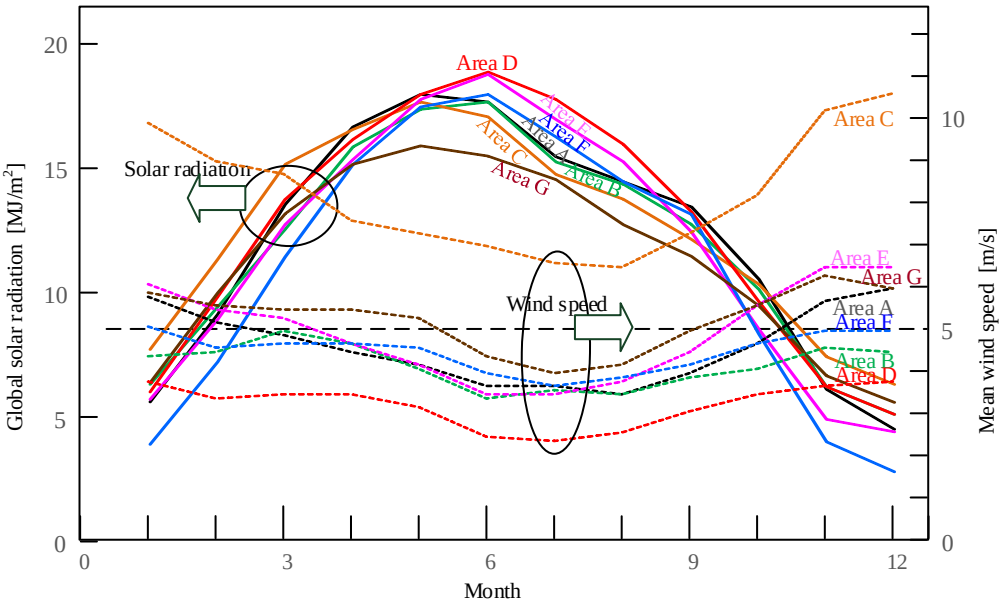

Fig. 6 The amount of global solar radiation and the mean wind speed for each Area

Figure 6 shows the amount of global solar radiation and the mean wind speed for each Area [35, 38]. As shown in the figure, global solar radiation is the highest from May to August, and the lowest in the winter months of November to February. In contrast, mean wind speeds are the highest during the winter months and the lowest in the summer season (July and August). Therefore, when solar and wind power stations are installed in the most suitable areas of Hokkaido, output fluctuations can be offset throughout the year.

4.1.2 Electrical demand

Figure 7 shows the total daily (24-hour) electrical demand for the seven areas of the Hokkaido region in February, June, and August. The power demand shown in the figure represents the sum total of the past electrical supply by an electric power utility [37] and the power demand of heat pump [38, 39]. Electricity for the entire Hokkaido region is currently supplied by an electric power company (Hokkaido Electric Power Co. Ltd.). In 2011, the company's portfolio of power sources included nuclear power (44%), thermal power (39%), hydroelectric power (15%), and renewable energy (2%).

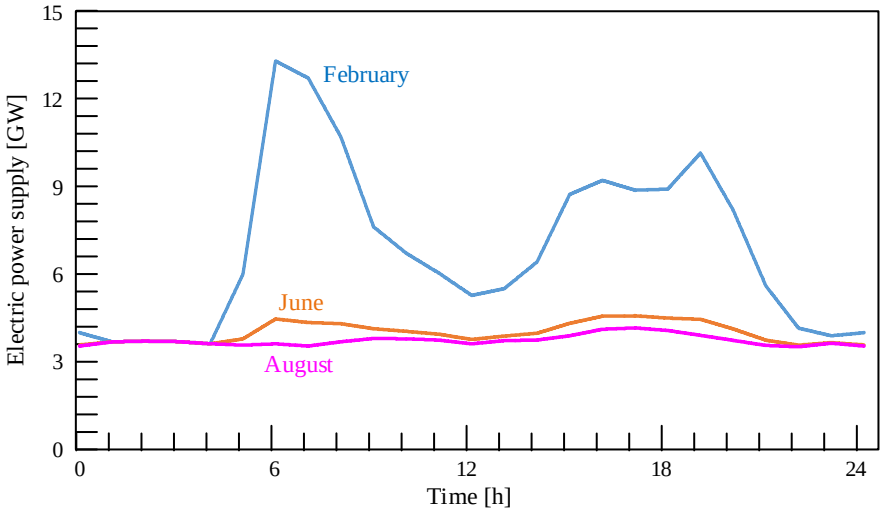

Fig. 7 Electric power demand

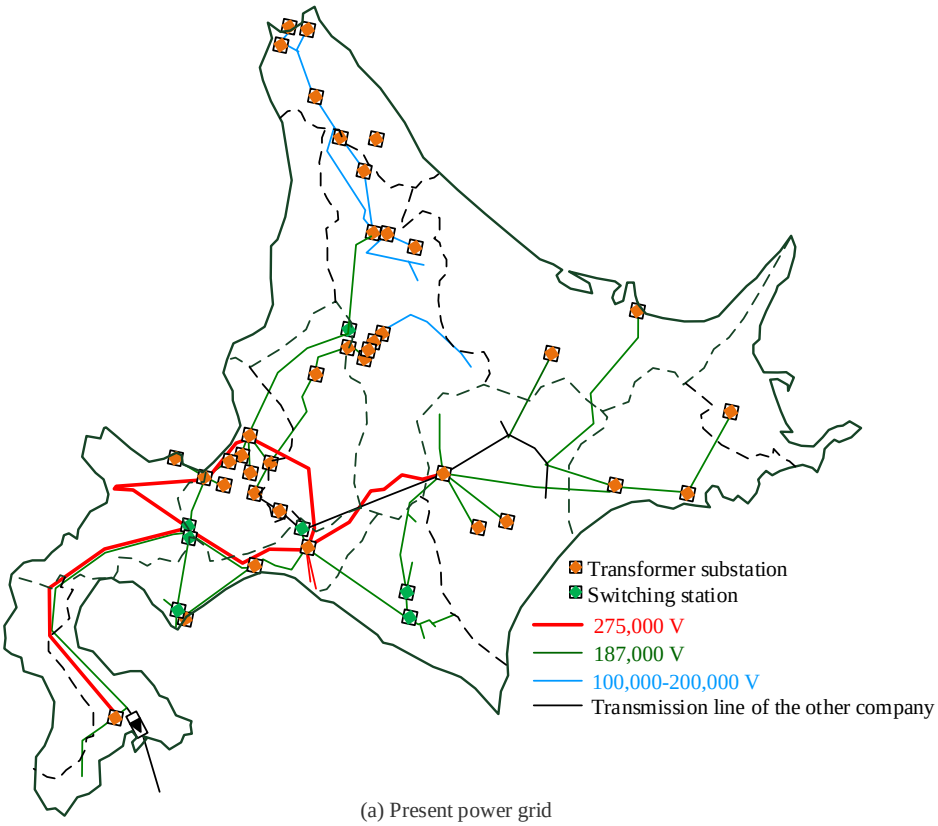

(a) Present power grid

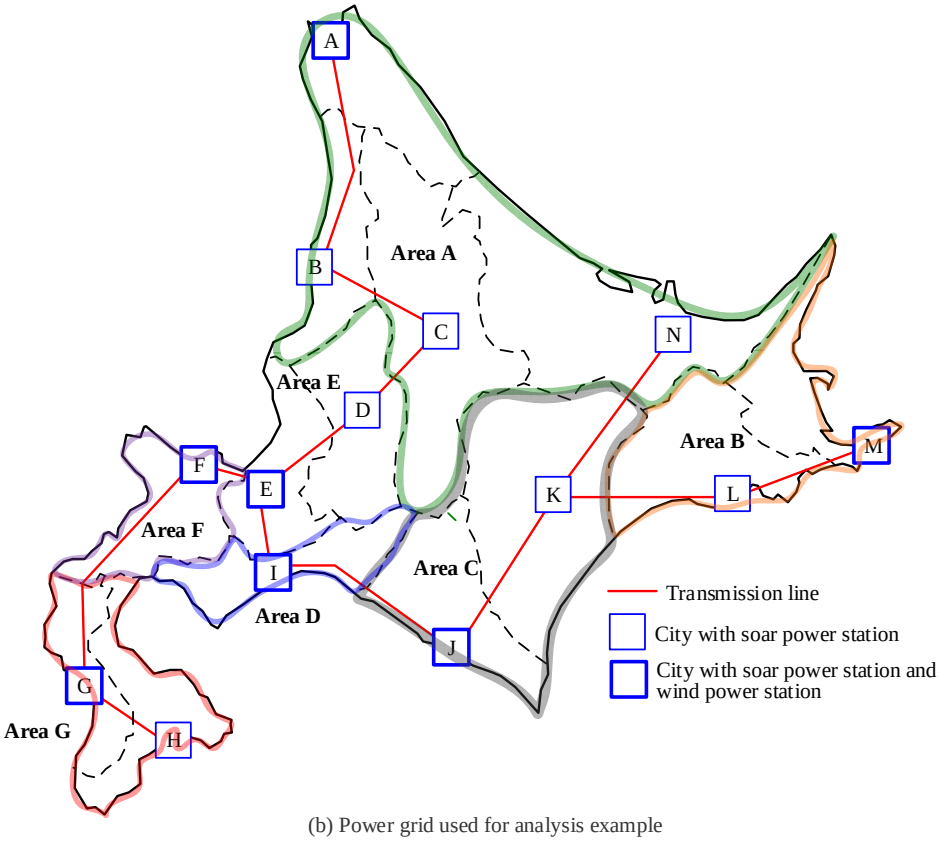

(b) Power grid used for analysis example

Fig. 8 Power grid in the Hokkaido region

4.1.3 The Hokkaido power grid

Figure 8(a) shows the current power grid for the Hokkaido region. Two or more large cities and industrial areas are included in Area A. In addition, one nuclear power station and at least two large-scale thermal power stations are currently located in the area. Only a small amount of renewable energy (2%) has been developed.

Figure 8(b) shows the seven areas selected for analysis (A through G) in this study. Within these selected areas, 14 cities (A through N) are identified as having existing solar or wind power stations. Solar power stations have been installed in all the cities (A through N). Wind power stations are installed in cities A, E, F, G, I, J, and M. In this study, the rated capacity of the renewable energy and CPS power sources and the cost of electrical delivery for solar and wind power between each area are clarified.

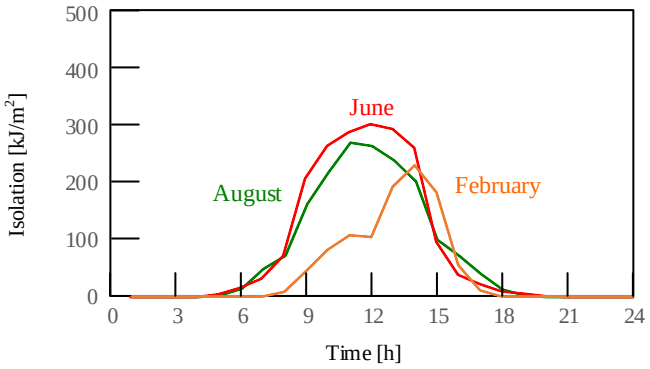

Fig. 9 24-hour data for the amount of global solar radiation in Sapporo (City E)

4.2 Distribution of renewable energy

4.2.1 Interconnection of solar power stations

Figure 9 shows 24-hour data for the amount of global solar radiation in Sapporo (City E) during February, June, and August [35]. When the existing solar power station installed in the range of several km is interconnected, as described in Section 2.2.2, the cyclic fluctuation of global solar radiation will be controlled to 20% or less of the rated power for less than 10 seconds. Therefore, this study utilizes random fluctuations of ±20% per 10 seconds. Global solar radiation with random fluctuations for cities A to N is shown in Appendix A. The conversion efficiency of solar cells used in the analysis was 18%.

4.2.2 Interconnection of wind power stations

A hypothetical wind power generator with the power curve shown in Fig. 10 is installed in each area. When numerous wind power stations arranged in the range of hundreds of km were interconnected, fringe fluctuations were 23% of the rated power. Therefore, for the purpose of this study, 23% of random fluctuations occur within 20 minutes. This result was used as the output pattern [36] for wind power generation.

4.3 Assumptions for the analysis

4.3.1 Pattern of electrical demand

The electricity demand pattern of cities A through N in Fig. 8 (b) is given in consideration of the population and space heating load of each city.

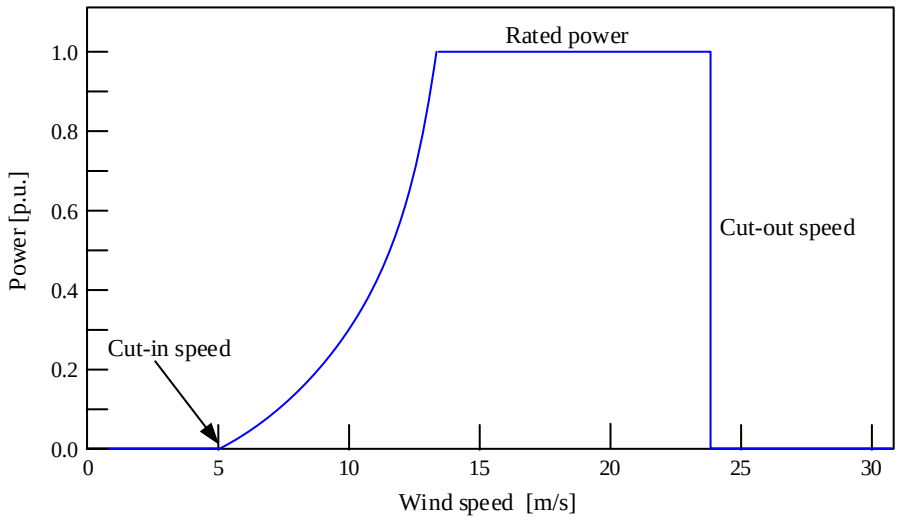

Fig. 10 Power curve of wind power generator

4.3.2 Cost of electrical power generation and delivery

This study used data from the Japanese government on generating costs (predicted values in 2030) [40] for various kinds of power sources. The power generation unit prices derived from that data are shown in Table 1. This study estimated the economic efficiency of the proposed system by introducing the values listed in Table 1 into Eq. (8).

The delivery costs in Table 1 refer to the example of a Japanese electric power company [41]. Although this study assumes that a liquid natural gas (LNG) combined cycle facility is the CPS backup supply; mean efficiency was estimated to be 30% considering partial loads during the operating period.

$$C_{gen,period} = \sum_{t=0}^{N_{period}} \sum_{r=1}^{N_{re}} \sum_{i=1}^{N_{area}} \left(u_{dp,r,i} \cdot p_{r,i,t} \cdot \Delta t \right) + \sum_{t=0}^{N_{period}} \left(u_{cps} \cdot p_{cps,t} \cdot \Delta t \right) \quad (8)$$

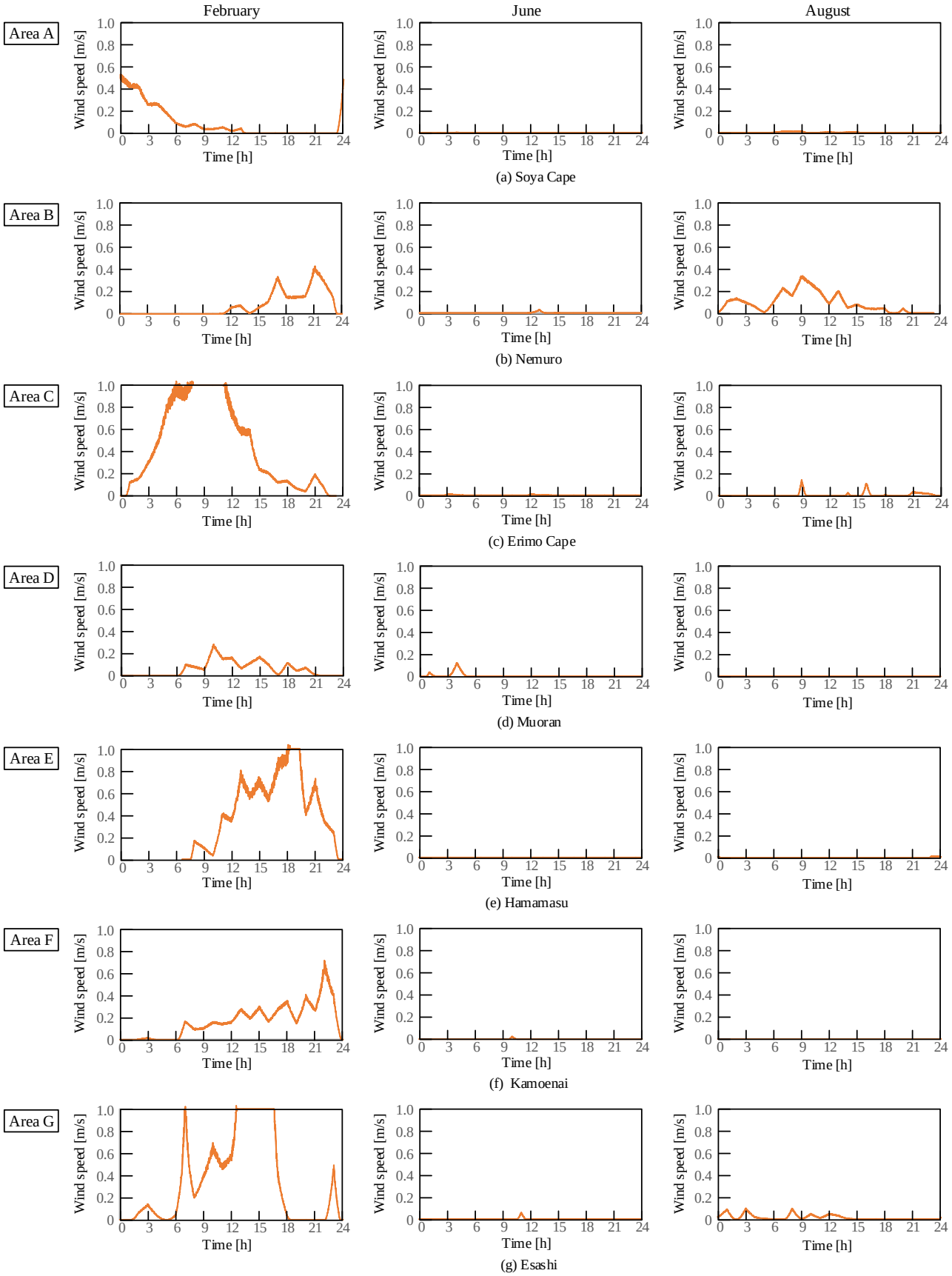

Fig. 11 Output of wind power generation of a representative day in each area

Table 1 Analysis conditions

CPS (Controllable Power Source of Output Power)	Natural gas combined cycle
Generating cost	110 USD/MW
Photovoltaics	
Generating cost	190 USD/MW
Wind power generator	
Power curve	Fig. 12
Generating cost	130 USD/MW
Delivery cost of electricity	38.1 USD/MW

Table 2 Parameters of genetic algorithm

Number of chromosomes	3000
Generation number	500
Interval of sampling time	60 sec
Probability of cross-over	20 %
Probability of mutation	20 %
Selection	
Individual with the maximum of adaptive value	15 % in all the individuals
Individuals with the 2nd to 5th place of adaptive value	5 % in all the individuals

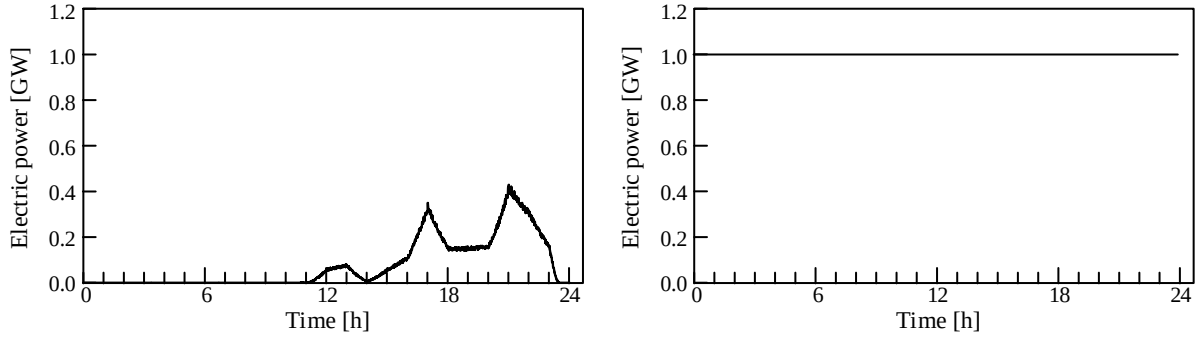

(a) Output of wind power station of Area B (Nemuro, February) (b) Load

Fig. 12 Output and load patterns of the wind power station

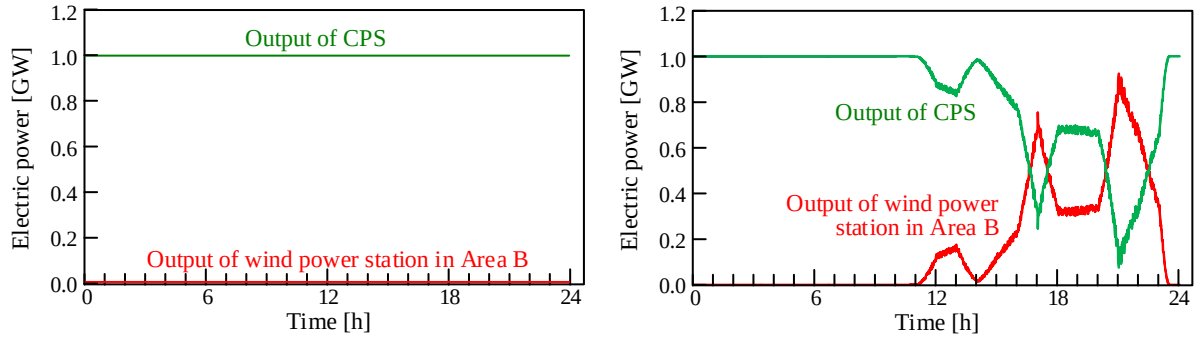

(a) Load is assumed in Area A (b) Load is assumed in Area B

Fig. 13 Analysis results for optimal operational planning using dummy data

4.3.3 Parameters and adaptive value of the GA

The parameters used for the GA are shown in Table 2. The values were determined by trial and error and extensive analytical calculations. Equation (8) evaluates economic efficiency. The objective function (adaptive value) uses Eq. (9) based on the objective function ((Eq. (7)) described in Section 3.4.1.

$$F_{system} = C_{gen,period} + C_{tp,period} \tag{9}$$

5. Results of Analysis

5.1 Operational analysis using dummy data

In this example, the power output of the solar power station and the wind power station was supplied to the power grid, as shown in Fig. 8(b). Then, the optimization analysis described in Section 4 was conducted. In this example, meteorological data and the complex load pattern of each city in the Hokkaido electric power system were used to estimate power output from the distributed renewable energy. Analysis of the results for optimization using the various data was difficult. Therefore, to investigate using the proposed analytic algorithm, simple dummy data for the output power of renewable energy and load patterns was provided.

Figures 12(a) and (b) show output and load patterns of the wind power station used for the analysis. The power output pattern for representative days in February was based on the wind power station installed in Nemuro (Fig. 11(b)) in Area B. On the other hand, assuming the demand of Area A or B, the load provided a steady state value, as shown in Fig. 12(b). Figure 13(a) shows the results when a case load occurs in Area A, and Fig. 13(b) shows the results when a case load occurs in Area B. When the power source and load are separated ((Fig. 13(a)), only

the CPS is planned. The reason is that the generation cost of the CPS is less than the renewable energy and delivery cost for transmitting electrical power from Area B to Area A. On the other hand, Fig. 13(b) shows results of the case in which the power source and load are in the same area. Although the generating cost of renewable energy is higher than the CPS (because there is no interchange of power between areas), operation of the wind power station is planned. The results of the optimization analysis based on the algorithm using the dummy data are shown in Fig. 13.

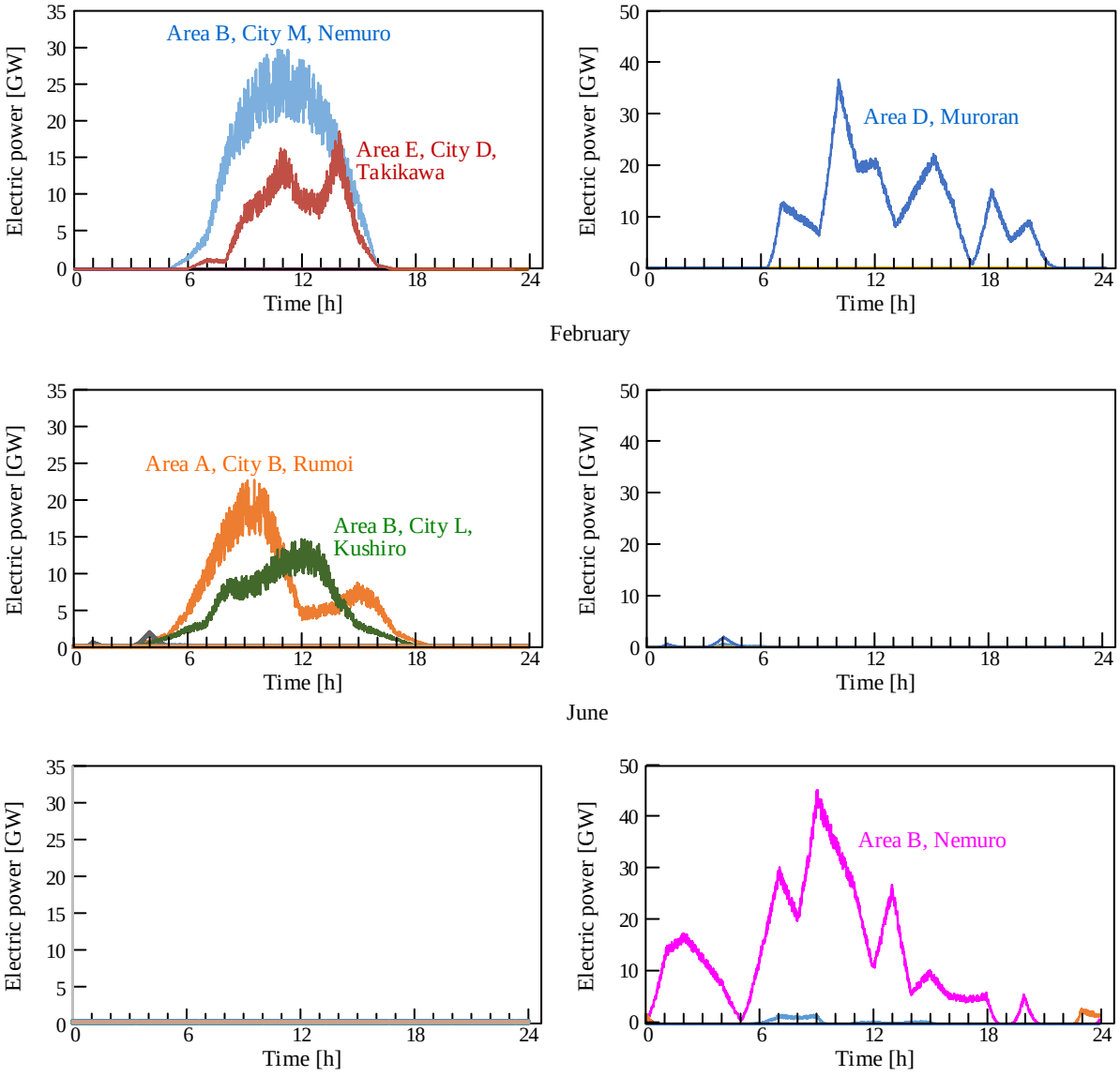

Fig.14 Power output of the solar power station for all the cities

5.2 Planning for installation of renewable energy in Hokkaido

5.2.1 Configuration of equipment

Figure 14(a) shows the power output of the solar power station for all the cities. Fig. 14(b) shows the output of the wind power station for all the cities. As shown in the figure, electrical power from both the solar power station and wind power station will be supplied in February. However, power will not be supplied by the wind power station in June or by the solar power station in August. Power generated by both the solar power stations will be supplied in February and June. Although the capacity and location of renewable energy affects the economic efficiency of the entire system, distribution of power from renewable energy to all the areas is not economically feasible. The reason is that renewable energy is more economically feasible under an intensive program for the installation of multiple power stations on an aggressive schedule.

Figure 15(a) shows the total demand for power from renewable energy that is interconnected with the transmission network. Data is displayed for February, June, and August. Figure 15(b) shows the corresponding power output of the CPS during the same duration. The figure shows the durations when significant amounts of existing, and possibly new, surplus power would be required. However, if the generating and delivery costs shown in Table 1 are used, installation of new renewable energy facilities with ample surplus power becomes feasible, as opposed to the construction of additional CPS backup supply facilities. Furthermore, because the cost of delivery will be added each time power is transferred to an area, development of new renewable energy can be planned at a reasonable pace, rather than intense development over a short period of time. The percentage of the total power load supplied by renewable energy on a representative day is projected to be 64.4% in February, 58.9% in June, and 80.6% in August. Based on the

results described above, it is expected through one year in whole Hokkaido that introduction of the renewable energy of a very high rate is possible.

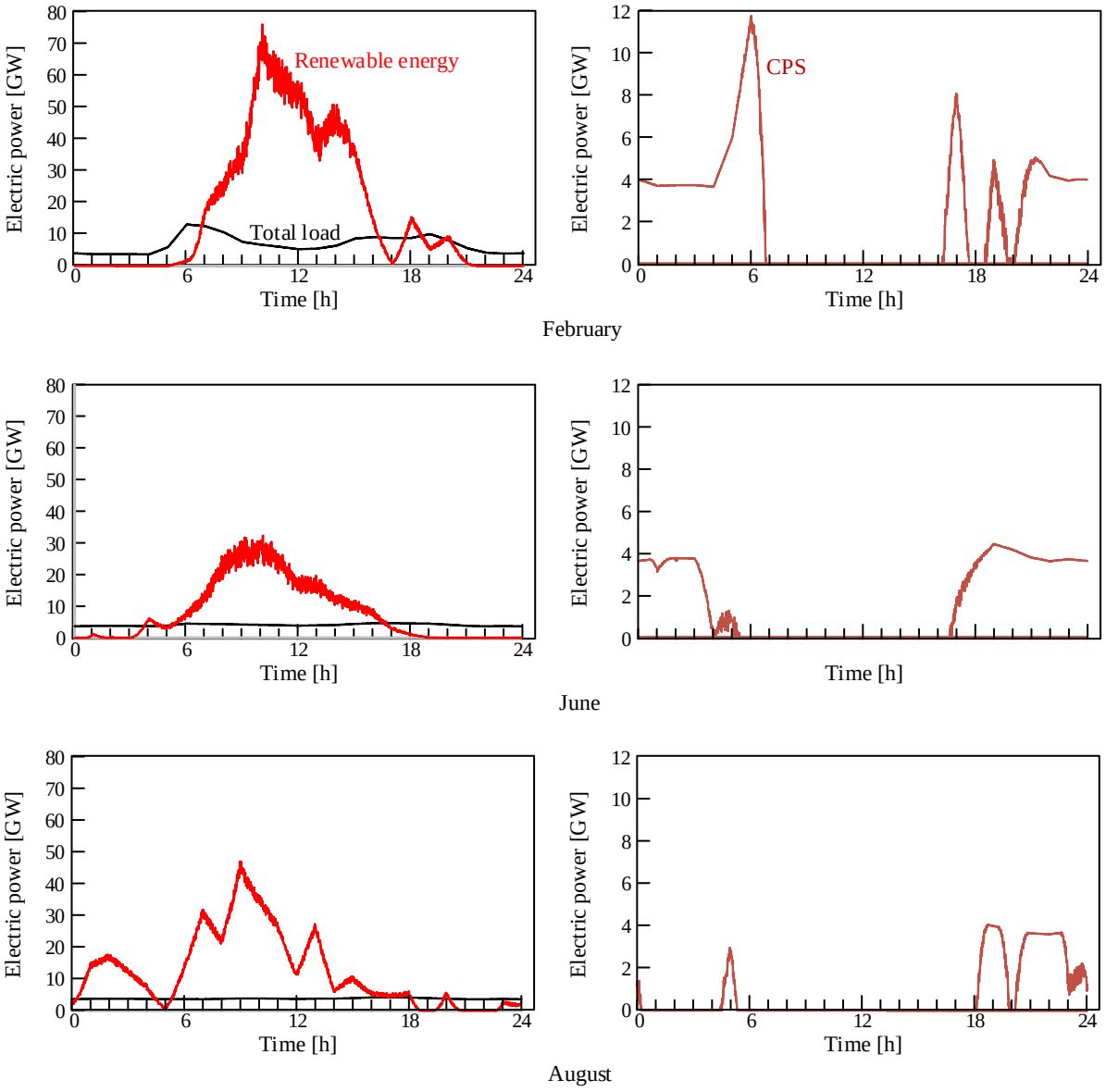

Fig. 15 Analysis results of total demand for power from renewable energy

5.2.2 Planning of equipment capacity

Figure 16 shows the projected installed capacity of wind and solar power stations for the cities in each area during February, June, and August. On the other hand, Fig. 17 shows the total

capacity of all the equipment for each of the three months. Because wind speeds in the Hokkaido region are higher in February, the supply of wind energy will increase and reduce the demand for backup power from the CPS. Because there is a time zone which will not be outputted from renewable energy in June and August, the rated capacity of the CPS is almost the same as the load peak of each month in Fig. 7.

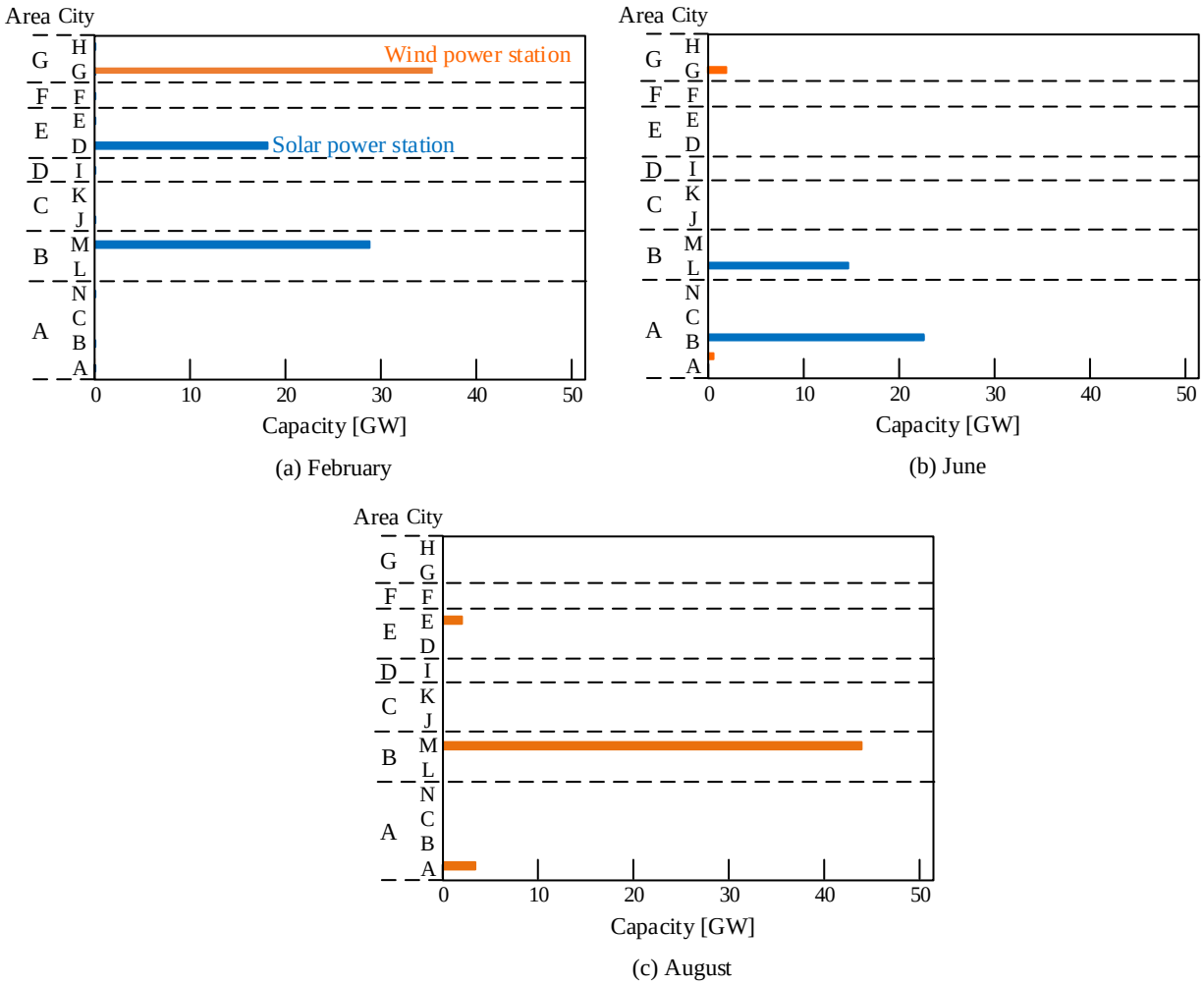

Fig. 16 Installed capacity of renewable energy in each area

Using the proposed algorithm, the capacity and efficiency of equipment and the required capacity of a backup power supply (CPS) can be analyzed. However, electricity storage is not considered in this study. When a fuel cell of suitable capacity is developed, an electrical power

system with a backup power supply sufficient to assure economic feasibility will possibly be constructed.

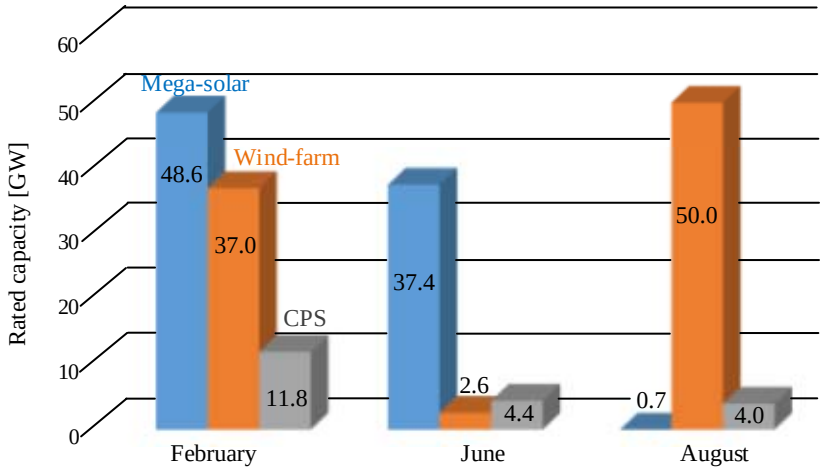

Fig. 17 Analysis results of total capacity of each equipment

6. Conclusions

In this study, a method for stabilizing the output of the electrical power grid was attained by interconnecting renewable energy facilities in areas where climate conditions differ. To clarify the type and capacity of renewable energy to be installed in each area, an optimization algorithm using a genetic algorithm was developed. The objective function of the optimization was to minimize facility and fuel costs of renewable energy facilities and the backup CPS, and facilitate the interchange and cost of power between areas.

As a result, the following conclusions were obtained.

(1) When the proposed algorithm is used, planning for equipment and facilities based on economic efficiency and the interconnection of renewable energy facilities over large areas is possible.

(2) When the renewable energy facilities are combined appropriately, the cost of the CPS (thermal power, hydroelectric power, etc.) will be significantly reduced. The location of renewable energy facilities in areas with suitable climatic conditions contributes to the stabilization of power distribution.

(3) When economic efficiency is part of the objective function for the interconnection of electrical power systems over large areas, fluctuations in power output that are characteristic of renewable energy can be planned for and offset through effective planning and design.

(4) Because the storage of electrical power was not considered in the proposed algorithm, it will be necessary to refine analytical methods for optimization when new and more efficient fuel cells are introduced in the future.

Glossary of Terms

C	:	Cost [USD]
C_{gen}	:	Cost of power generation [USD]
F_{system}	:	Objective function of the system
l	:	Transportation distance [km]
N	:	Number
p	:	Power [MW]
Δp	:	Loss of power [MW]
Δp_{tp}	:	Amount of power transmission [MW]
r_{pf}	:	Rate of output fluctuation [%]
t	:	Sampling time [s]

Δt : Interval of sampling time [s]

USD : U.S. dollar

u : Unit price of equipment [USD/MW]

u_{dp} : Provisional estimate by the Japanese government of the unit price for the production of electricity [USD/MW]

u_{dv} : Unit price for delivery of electricity [USD/MWh]

V : Rated capacity [MW]

v : Fuel consumption [MW]

Greek characters

$\bar{\eta}$: Mean efficiency for the production of electricity

λ_{loss} : Loss factor

Subscript

area : Introductory area of a power source

CPS : Controllable source of power output

need : Power demand

pv : Solar power station

re : Renewable energy

tp : Power transmission

wp : Wind power station

Appendix A

Figures A.1 and A.2 shows global solar radiation with random fluctuations for cities A through N in Hokkaido, Japan. These data was used for the analysis of this paper.

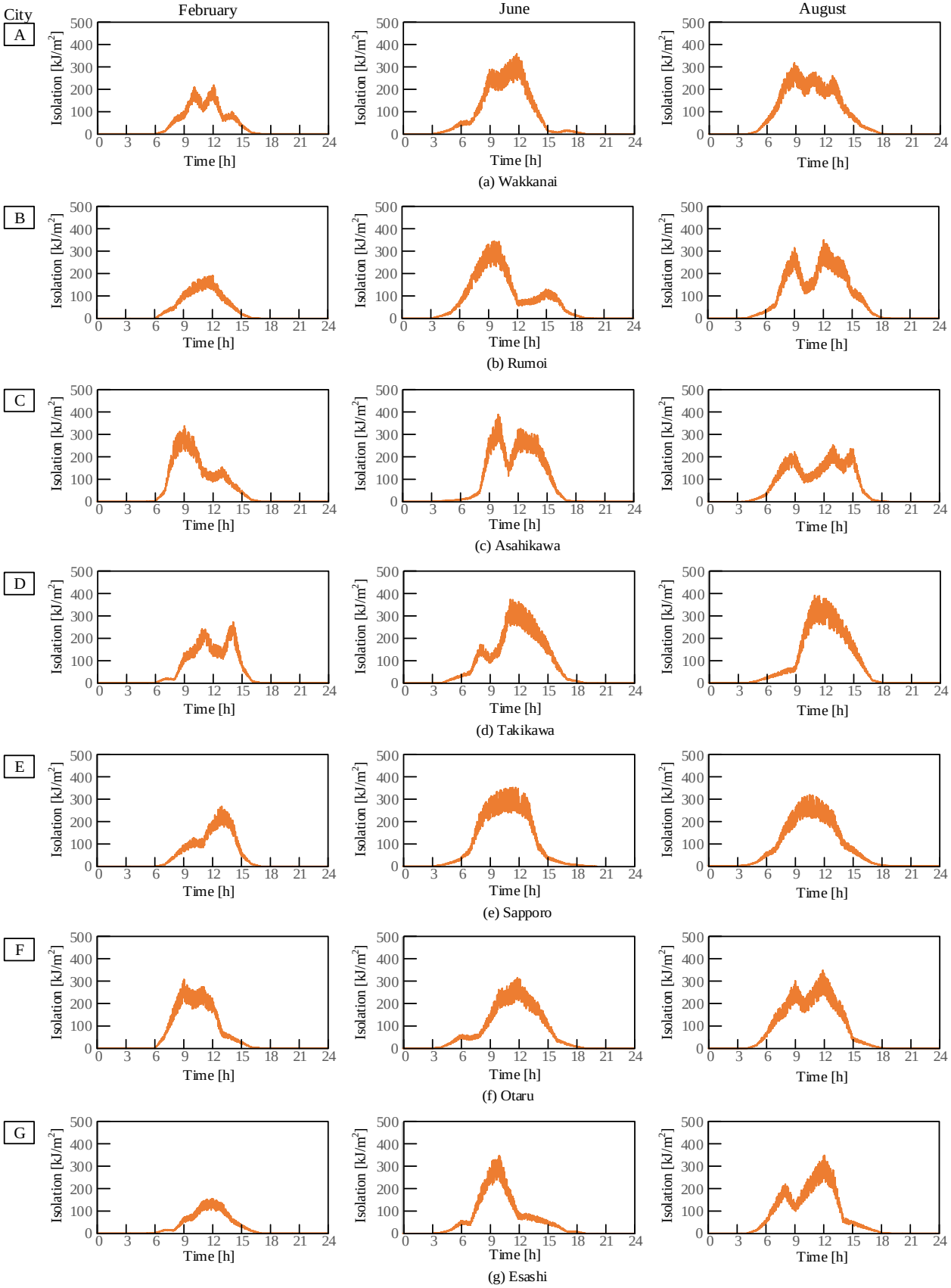

Fig. A.1 Global solar radiation with random fluctuations for Each city (cities A through G)

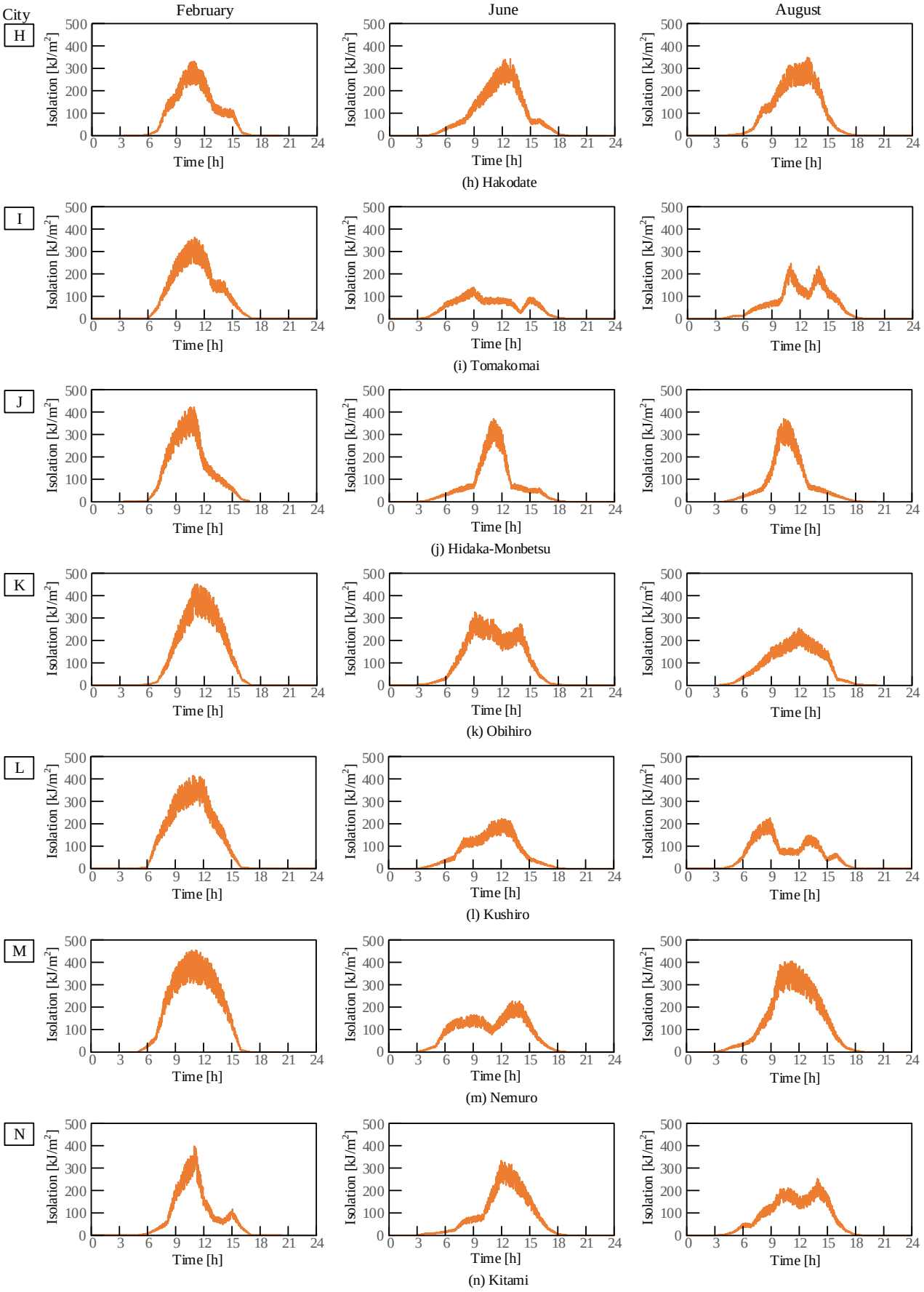

Fig. A.2 Global solar radiation with random fluctuations for Each city (cities H through N)

References

[1] Kinney R, Crucitti P, Albert R, Latora V, Modeling cascading failures in the North American power grid. The European Physical Journal B–Condensed Matter and Complex Systems 2005:46;101–107.

[2] Short J A, Infield D G, Freris L L, Stabilization of grid frequency through dynamic demand control. Transactions on Power Systems, IEEE 2007:22;1284–1293.

[3] Carrasco J M, Franquelo L G, Bialasiewicz J T, Galvan E. Guisado R C P, Prats M A M, Leon J I, Moreno–Alfonso N, Power–electronic systems for the grid integration of renewable energy sources: a survey. Industrial Electronics, IEEE 2006:53;1002–1016.

[4] Roozbehani M, Dahleh M, Mitter S, Dynamic pricing and stabilization of supply and demand in modern electric power grids. First IEEE International Conference on Smart Grid Communications (SmartGridComm) 2010:543–548.

[5] Bao J, Bao W, Gong J, A PWM multilevel current–source inverter used for grid–connected wind energy conversion system. Energy Procedia, Part A 2012;16:461–466.

[6] Ruiz–Romero S, Colmenar–Santos A, Mur–Pérez F, López–Rey Á, Integration of distributed generation in the power distribution network: The need for smart grid control systems, communication and equipment for a smart city—Use cases. Renewable and Sustainable Energy Reviews 2014;38:223–234.

[7] Hassan L, Moghavvemi M, Almurib H, Muttaqi K, Ganapathy V, Optimization of power system stabilizers using participation factor and genetic algorithm. International Journal of Electrical Power & Energy Systems 2014;55:668–679.

[8] Voyant C, Darras C, Muselli M, Paoli C, Nivet M, Poggi P, Bayesian rules and stochastic

models for high accuracy prediction of solar radiation. Applied Energy 2014;114:218–226.

[9] Kwon P, Østergaard P, Assessment and evaluation of flexible demand in a Danish future energy scenario. Applied Energy 2014;134:309–320.

[10] Divya K, Østergaard J, Battery energy storage technology for power systems—An overview, Electric Power Systems Research 2009;79:511–520.

[11] Kawakami N, Iijima Y, Sakanaka Y, Kawakami N, Fukuhara M, Ogawa K, Bando M, Matsuda T., Development and field experiences of stabilization system using 34 MW NAS batteries for a 51 MW wind-farm. IEEE International Symposium on Industrial Electronics (ISIE) 2010;2371–2376.

[12] Hill C A, Such M C, Chen D, Gonzalez J, Grady W M, Battery energy storage for enabling integration of distributed solar power generation. IEEE Transactions on Smart Grid 2012;3: 850–857,

[13] Bragard M, Soltau N, Thomas S, Doncker R W, The balance of renewable sources and user demands in grids: power electronics for modular battery energy storage systems. IEEE Transactions on Power Electronics 2010;25:3049–3056.

[14] Tong S, Same A, Kootstra M, Park J, Off–grid photovoltaic vehicle charge using second life lithium batteries: An experimental and numerical investigation. Applied Energy 2013;104:740–750.

[15] Arghandeh R, Woyak J, Onen A, Jung J, Broadwater R., Economic optimal operation of Community Energy Storage systems in competitive energy markets. Applied Energy 2014;135:71–80.

[16] Konishi R, Takahashi M, Optimal allocation of photovoltaic systems and energy storages in

power systems considering power shortage and surplus. Electric Power Quality and Supply Reliability Conference, IEEE 2014;127–132.

[17] Franco A, Salza P, Strategies for optimal penetration of intermittent renewables in complex energy systems based on techno-operational objectives. Renewable Energy 2011;36:743–753.

[18] Obara S, Kawai M, Kawae O, Morizane Y, Operational planning of an independent microgrid containing tidal power generators, SOFCs, and photovoltaics. Applied Energy 2013;102:1343–1357.

[19] Kanchev H, Lu D, Colas F, Lazarov V, Francois B, Energy management and operational planning of a microgrid with a PV-based active generator for smart grid applications. IEEE Transactions on Industrial Electronics 2011;58:4583–4592.

[20] Zeng M, Duan J, Wang L, Zhang Y, Xue S,Orderly grid connection of renewable energy generation in China: Management mode, existing problems and solutions. Renewable and Sustainable Energy Reviews 2015;41:14-28.

[21] Reddy K S, Kumar M, Mallick T K, Sharon H, Lokeswaran S, A review of Integration, Control, Communication and Metering (ICCM) of renewable energy based smart grid. Renewable and Sustainable Energy Reviews 2014;38:180-192.

[22] Ramirez D, Martinez S, Carrero C, Platero A C, Improvements in the grid connection of renewable generators with full power converters. Renewable Energy 2012;43:90-100.

[23] Connollya D, Lundb H, Mathiesenb B, Picana E, Leahya M, The technical and economic implications of integrating fluctuating renewable energy using energy storage. Renewable Energy 2012;43:47–60.

[24] Li Q, Choi S S, Yuan Y, Yao D L, On the determination of battery energy storage capacity

and short-term power dispatch of a wind-farm. IEEE Transactions on Sustainable Energy 2011;2:1949–3029.

[25] Yao D L, Choi S S, Tseng K J, Lie T T, Determination of short-term power dispatch schedule for a wind-farm incorporated with dual-battery energy storage scheme. IEEE Transactions on Sustainable Energy 2012;3:74–84.

[26] Control strategies to smooth short-term power fluctuations in large photovoltaic plants using battery storage systems. 2014;7:6593–6619.

[27] Haaren R, Morjaria M, Empirical assessment of short-term variability from utility-scale solar PV plants. Progress in Photovoltaics: Research and Applications 2014;22:548–559.

[28] Li J H, Zhu X X, Yan G G, Mu G, Luo W H, Design of energy storage station grouping energy management strategies to balance short-term wind power fluctuations. Applied Mechanics and Materials 2013;2866–2871.

[29] Output fluctuation and alleviation method of PV, The National Institute of Advanced Industrial Science and Technology (AIST) of Japan, Retrieved from https://unit.aist.go.jp/rcpvt/ci/about_pv/output/fluctuation.html;2014

[30] Check working group of the interconnection possible quantity of wind power generation, The calculation process of the interconnection possible quantity of wind power generation (Tohoku Electric Power). Electric Power System Council of Japan (ESCJ) 2011;1–66. In Japanese

[31] Abd-El-Waheda W F, Mousab A A, El-Shorbagyb M A., Integrating particle swarm optimization with genetic algorithms for solving nonlinear optimization problems. Journal of Computational and Applied Mathematics 2011;235:1446–1453.

[32] Tang K Z, Sun T K, Yang J Y, An improved genetic algorithm based on a novel selection

strategy for nonlinear programming problems. Computers & Chemical Engineering 2011;35:615–621.

[33] Lia L, Mua H, Gaob W, Li M, Optimization and analysis of CCHP system based on energy loads coupling of residential and office buildings. Applied Energy 2014;136:206–216.

[34] Yu F, Xu X, A short-term load forecasting model of natural gas based on optimized genetic algorithm and improved BP neural network. Applied Energy 2014;134:102–113.

[35] Annual amount-of-insolation data base (METPV-11), New Energy and Industrial Technology Development Organization (NEDO), http://www.nedo.go.jp/library/nissharyou.html;2014.

[36] The past meteorological data, Information of the climatological statistics, Japan Meteorological Agency, http://www.data.jma.go.jp/obd/stats/etrn/;2014.

[37] Electricity status-of-use data in 2010, The past electricity status-of-use data, Hokkaido Electric Power Co., Inc., http://denkiyoho.hepco.co.jp/download.html;2014

[38] Analysis of the actual condition of the energy consumption of the private sector of Hokkaido, Investigation on the energy problems of Hokkaido by immediate job creation promotion task, Hokkaido Government 2014;162:1–62;

[39] The development of the CO_2 heat pump hot water supply unit for business use that can be operated down to -25 degrees Celsius of outside air temperature. Technical report, Mitsubishi Heavy Industries Co., Ltd. 2011;48:86–88.

[40] Generating cost of each power-source (2004 trial calculation / 2010 and 2030 model plant), Report of the examination committee of cost, Energy and environmental conference of Japanese government 2013;62. In Japanese

[41] The official announcement of the market price of national accommodation, etc., The past

meteorological data, Information of the climatological statistics, Kyushyu Electric Power, http://www.kyuden.co.jp/company_liberal_yutsu.html;2014. In Japanese